PROCEEDINGS, Thirty-Sixth Workshop on Geothermal Reservoir Engineering
Stanford University, Stanford, California, January 31 - February 2, 2011
SGP-TR-191

LABORATORY EXPERIMENTAL STUDY OF HEAT EXTRACTION FROM POROUS MEDIA BY MEANS OF CO_2

Mario Magliocco[1,2], Timothy J. Kneafsey[2], Karsten Pruess[2], and Steven Glaser[1,2]

[1]Department Civil and Environmental Engineering
University of California, Berkeley, CA 94720
[2]Lawrence Berkeley National Laboratory
Berkeley, CA 94720
e-mail: mag@berkeley.edu

ABSTRACT

The use of CO_2 as a heat transfer fluid has been proposed as an alternative to water in enhanced geothermal systems (EGS). Numerical simulations have shown that under expected EGS operating conditions, CO_2 could achieve more efficient heat extraction performance than water. We have conducted laboratory experiments with dry supercritical CO_2 in order to test and refine the theoretically derived heat transfer predictions. We have injected cold CO_2 into heated porous media held in a laboratory pressure vessel, and have monitored temperature changes at different locations. To date, our measurements cover a pressure range from 77 to 120 bar, temperatures from 20 to 77°C, and a range of CO_2 injection rates. Temperature data recorded at different thermocouple locations capture behavior that ranges from broad diffusion-dominated transients at low flow rates to sharp temperature breakthrough curves when conditions are advectively dominated (high-Peclet number). Numerical simulations with TOUGH2/ECO2N using a 2-D axisymmetric model agree reasonably well with the experimental measurements.

The laboratory tests have demonstrated the technical challenges involved in working with supercritical CO_2, which are due to the sensitivity of the fluid's physical properties to subtle changes in operating conditions. The results of our experiments and simulations will provide useful guidance as we develop a more capable experimental apparatus.

INTRODUCTION

Geothermal energy is a vast and largely untapped resource that, if efficiently utilized, could satisfy the majority of the base load energy demand in the United States (Tester et al., 2006). Current commercial geothermal electricity production is dependent on a number of factors including an optimized combination of geological conditions such as presence of hydrothermal fluid, high heat flux, high rock permeability and/or high rock porosity. Enhanced (or Engineered) Geothermal systems (EGS) are an attempt to exploit geothermal energy in locations where these conditions are not optimal (Tester et al., 2006). Most EGS strategies involve reservoir stimulation to overcome the lack of porosity and/or permeability of the rock using various chemical and physical processes, as well as supplying the needed heat transfer process fluid (Majer et al, 2007).

The novel concept of using supercritical CO_2 (SCCO2) as the working fluid in EGS for both reservoir creation and heat extraction was first proposed by Brown (2000). Subsequent work includes numerical simulations of a five-spot well pattern in a hot dry rock (HDR) system, which estimated an approximately 50% greater heat extraction rate using SCCO2 instead of water, given the same operating conditions (Pruess, 2006). The advantages of using CO_2 over water as the process fluid in a closed loop HDR system include (1) much lower viscosity of CO_2 means that substantially larger mass flow rates can be achieved for a given pressure drop between injection and production points; (2) much larger density difference between cold fluid in the injection well and hot fluid in the producer means increased buoyancy forces for CO_2, which will reduce or even eliminate pumping requirements; (3) lower mineral reactivity of dry SCCO2 would reduce equipment fouling, and reduce the possibility of dissolution and precipitation reactions that could negatively impact the reservoir quality; and (4) hotter reservoirs could be developed without silica dissolution problems present in water based systems. As an ancillary benefit, practical operation of a SCCO2 system would result in de facto carbon

sequestration due to fluid loss to the surrounding formations (Brown, 2000, Pruess 2006). In light of the promising results of both thermodynamic and chemical simulations (Pruess and Spycher 2010; Xu and Pruess 2010), it is necessary to confirm the theoretical work with practical laboratory and field experiments.

This paper presents the design, implementation, and results of a laboratory-scale SCCO2-based heat extraction experiment with the goal of verifying and validating the modeling tools and theoretical predictions, and improving the design of an experimental system.

EXPERIMENT DESCRIPTION

Theoretical Considerations

Building confidence in numerical modeling tools requires experimental studies performed over a range of conditions represented by the simulator, ensuring sufficient control of experimental conditions, and measuring those aspects that are not controlled so that the system can be effectively simulated. For the reported experiment, we used the TOUGH2 numerical simulator (Pruess, 2004) in combination with the "ECO2N" fluid property module that was designed to study CO_2 sequestration in saline aquifers (Pruess and Spycher, 2007). The underlying TOUGH2 equations are based on the assumption that the fluid flow is within the Darcy regime. To ensure that we operate the experiment in the Darcy flow regime, the flow conditions are characterized by a Reynolds number (Re) that should be less than 10 (Bear 1972). The Reynolds number for fluid flow through a packed bed, e.g. a sand pack with average grain size d_{50}, can be defined by Equation 1:

$$\mathrm{Re} = \frac{v \rho_f d_{50}}{\mu} \quad (1)$$

where v is the pore velocity, ρ_f is the fluid density, and μ is the dynamic viscosity of the fluid (Freeze and Cherry 1979).

The large differences in temporal and spatial scales between field and laboratory conditions make it impossible for a laboratory-scale experiment to fully represent field scale. The interplay between advective and conductive heat transport is described by the Peclet number (Pe) which provides a useful tool to highlight the differences. The Peclet number (Equation 2) can be expressed as the ratio of the time required for both processes to pass across the length scale in question (i.e. conduction time over advection time).

$$\mathrm{Pe} = \frac{t_{cond}}{t_{ad}} = \frac{L^2 / D_{th}}{L / V_p} = \frac{L V_p}{D_{th}} \quad (2)$$

In Equation 2, t_{cond} is the characteristic thermal conduction time, t_{ad} is the characteristic advection time, D_{th} is the thermal diffusivity, L is the characteristic length, and V_p is the pore velocity. The parameters for calculating the thermal diffusivity of the laboratory system are given below (Table 1).

Table 1: Design Case System Properties

Porous Core Properties	
length (distance to farthest TC)	L_{tc} = 28.1 cm
total core length	L = 50.8 cm
cross sectional area	A = 6.54×10^{-3} m^2
grain density	ρ_R = 2600 kg/m^3
grain specific heat	C_R = 920 J/kg/ □C
rock thermal conductivity	K = 2.51 W/m/ □C
permeability	k = 9.3×10^{-13} m^2
porosity	□ = 41%
mean grain size d_{50}	$d_{50} \approx$ 0.130 mm
Test Conditions	
core temperature	$T_f \approx$ 65°C
core pressure	P ≈ 10 MPa
pump temperature	$T_P \approx$ 13°C
CO_2 Properties at Test Conditions	
viscosity	μ = 2.3×10^{-5} Pa·s
density (in sample)	ρ_f = 266 kg/m^3
density (in pump)	ρ_P = 903 kg/m^3

Thermal diffusivity for both systems is $D_{th} = K/(\rho_R C_R) = 1.05 \times 10^{-6}$. The Peclet number for the field system simulated in (Pruess, 2006) is on the order of 6.62×10^5. Assuming an identical pore velocity, the Peclet number for the lab system would be about three orders of magnitude smaller due to the differences in length. Achieving a similar Peclet number on the lab scale requires increasing the pore velocity of the system. A limit on the pore velocity is imposed by maintaining the Reynolds number below 10.

The Darcy velocity (or volumetric flux) is $v = Q_v/A$ where Q_v is the volumetric flow rate in the vessel. The volumetric flow rate in the vessel is related to the volumetric flow rate in the pump, Q_P, by a ratio of the densities at the two locations. Using these relationships the pore velocity can be expressed as:

$$V_p = \frac{v}{\phi} = \frac{Q_V}{A\phi} = \frac{Q_P\rho_P}{A\phi\rho_f} \quad (3)$$

Where ρ_p is the density of the fluid in the pump, and ρ_f is the density of the fluid in the vessel (at initial conditions). Using equation 3 and equation 1, we can express a relationship between the volumetric flow rate from the pump and the Reynolds number:

$$Re = \frac{Q_P\rho_P d_{50}}{A\mu} \quad (4)$$

The relevant properties are listed in Table 1.

At the assumed test conditions the maximum Reynolds number of 10 would correspond to a maximum volumetric flow rate at the pump of $Q_P = 1.28\text{x}10^{-5}$ m^3/s = 769 ml/min, which is well beyond the flow rating of our laboratory pumps. Our maximum practical flow rate is 175 mL/min at pump conditions. A flow rate of 175 mL/min at the assumed test conditions results in Pe = 988 which is about three orders of magnitude smaller than for a field system.

A final design consideration is the large buoyant effects of SCCO2. It has been shown that even for small length scales, buoyant effects of SCCO2 can have a large effect on the dynamics of an SCCO2-based system (Liao and Zhao 2002). For a horizontal flow arrangement, buoyant forces can result in pressure gradients that are oriented perpendicular to the vessel axis, complicating the dynamics. For modeling and comparison purposes, it is simpler to align the flow path in the same orientation as the gravity-induced pressure gradient.

Experimental Apparatus

Our vessel consists of a hollow stainless steel cylinder with an inside diameter of 9.124 cm, outside diameter of 12.7 cm, 50.8 cm distance between the end caps, and a pressure safety rating of 34.5 MPa (345 bar, 5000 psi). Instrumentation access to the interior of the vessel is through three axial passages through one end cap, and one passage on the other. The central passages through the end caps are used as the injection and production ports and the remaining two passages are used exclusively for temperature sensing (Figure 1). All temperature measurements were made using 1.59 mm diameter stainless-steel clad type-T thermocouples.

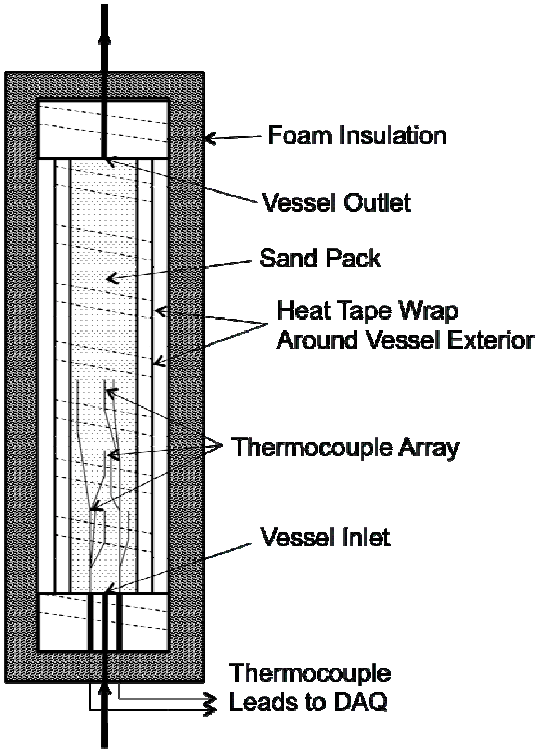

Figure 1: Vessel setup detail.

The injection port was lined with a length of nylon tubing in order to provide thermal insulation for the injected fluid as it passes through the relatively massive end cap. The injection port was also fitted with a single thermocouple mounted where the injected fluid enters the sample space. Stainless steel wire gauze and a fine screen were used at either end of the vessel to prevent the porous medium from migrating out of the vessel during operation.

The vessel was dry packed with F110 Ottawa silica sand (US Silica) in multiple lifts. Thin foam rubber discs were placed on either end of the sand pack to provide a small amount of axial load to the sample and thereby avoid creating a void space in the media after the end caps were secured. The vessel was then wrapped with two 1.8-meter lengths of heat tape that extended around the exterior of the end caps. The heater temperature was controlled by a PID controller using a thermocouple secured on the vessel exterior underneath the heat tape wrap as the feedback. Finally the vessel was wrapped in foam insulation and sealed.

Nine TCs were located within the vessel, one at the inlet, and 8 located within the core at three different

distances from the injection point along the axis (13.3 cm, 20.8 cm, and 28.3 cm), and at three different radii measured from core axis (0 cm, 1.52 cm and 3.04 cm, Figure 2). The radial symmetry of the system allowed the thermocouples to be placed such that they were not all aligned to reduce axially preferential flow paths along the thermocouple exterior.

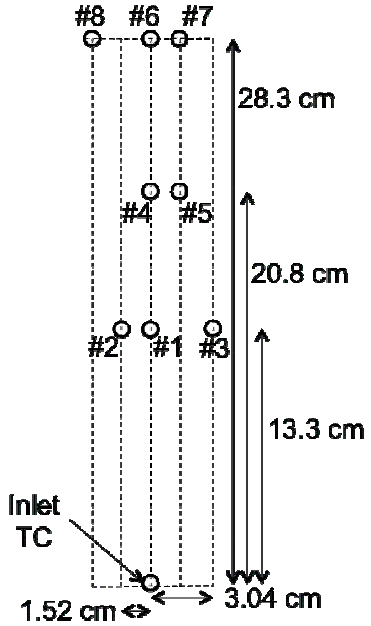

Figure 2: Thermocouple array geometry and numbering scheme (to scale).

A sketch of the experimental system is shown in Figure 3. Fluid pressure and storage is provided by three high-pressure syringe pumps: two externally cooled Isco 500D pumps for fluid injection and flow rate control, and a single Isco 1000D pump to store the fluid exiting the vessel until it could be used to refill the injection pumps. The pumps and all valves were controlled manually. After the fluid exits the injection pumps, it passes through a heat exchanger before entering the vessel to ensure a stable fluid injection temperature. Initial scouting runs indicated that a second heat exchanger was required in the return flow path to the 1000D pump because the fluid volume expansion upon leaving the heated vessel overwhelmed the fluid storage capacity of the system. The injection pumps and the heat exchangers were both fed coolant from a recirculating laboratory chiller set at 5°C.

Backpressure at the outlet side of the vessel was provided by a backpressure regulator, either controlled by fluid pressure from an additional high-pressure syringe pump or a Tescom 300ER digital PID pressure regulator. Both regulating schemes were prone to noise in their output, but the PID was more stable over a larger range of fluid states. For lower flow rates with a smaller range of fluid states, the non-PID controlled setup was more stable.

Temperature was also measured on the vessel exterior, within the flow path immediately downstream of the injection pumps, the exterior of the pump cylinders, and at the output of the test vessel. Independent measurements of pressure were made at both ends of the vessel, as well as the pressure differential across the vessel. The volumetric flow rates, and pressures as reported by the pump controllers were also recorded.

Experiment Procedure

The system was leak tested and filled with dry CO_2. After heating the sand-packed vessel to the desired

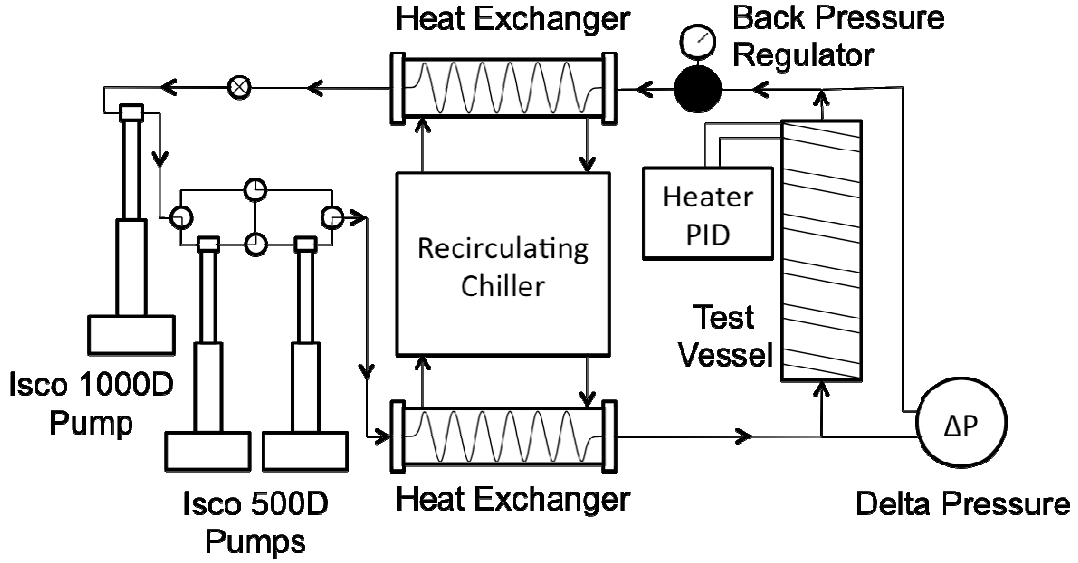

Figure 3: Flow and control schematic of the experimental apparatus.

operating temperature, anhydrous fluid CO_2 was added or removed to achieve the desired operating pressure, and the apparatus was allowed to thermally equilibrate overnight. At this point the backpressure was set to the desired pressure and cold liquid CO_2 injected into the bottom of the vessel at a prescribed volumetric flow rate. The collection pump maintained a constant pressure, smaller than the backpressure value so it could collect fluid exiting the regulator. When the first injection pump approached the end of its cycle, the second injection pump was activated, allowing the first pump to be refilled from the fluid collection pump. The injection pumps were cycled in this manner until the experimental run was completed with 4 to 8 pump volumes of fluid injected (2 to 4 L) per run.

EXPERIMENTAL RESULTS

Figure 4 presents the temperatures at the various thermocouple locations for a typical experimental run. Before the fluid is injected the vessel is near thermal equilibrium with the room and the heater tape. The start of fluid injection can be clearly seen by the initial steep temperature drop at the inlet location. Note significant axial temperature gradients in the vessel before fluid injection begins, with a higher temperature at the top of the vessel than at the injection point at the bottom.

Once the flow of cold fluid begins, a small perturbation can be seen at all of the TC locations in the core, which indicates a small simultaneous short-term increase in temperature. This feature was present in all of our experimental runs. The temperature front can be seen in the plot as it passes axially through the sample past the TC locations. After the initial sharp temperature drop, the temperatures gradually approach equilibrium, and a radial temperature gradient then develops, indicated by the grouped lines spreading out. The exterior locations (dot-dashed lines) trend towards a higher temperature than those that are more central (solid lines). The small spikes in the inlet temperature profile indicate the injection pump switch events which take several tens of seconds to complete, during which time the injected fluid became hotter due to a longer residence time in the end cap. In the test shown in Figure 4, the temperatures at the thermocouples located closest to the injection point reach a temperature minimum before increasing again and reaching equilibrium. This local minimum did not occur in all experimental runs. The rise of the temperatures after the minima is most likely related to the increase in injection fluid temperature as the warmer recirculated fluid reentered the vessel.

Our test pressures ranged from 77 to 120 bar, temperatures from 20 to 77°C, and the flow rates

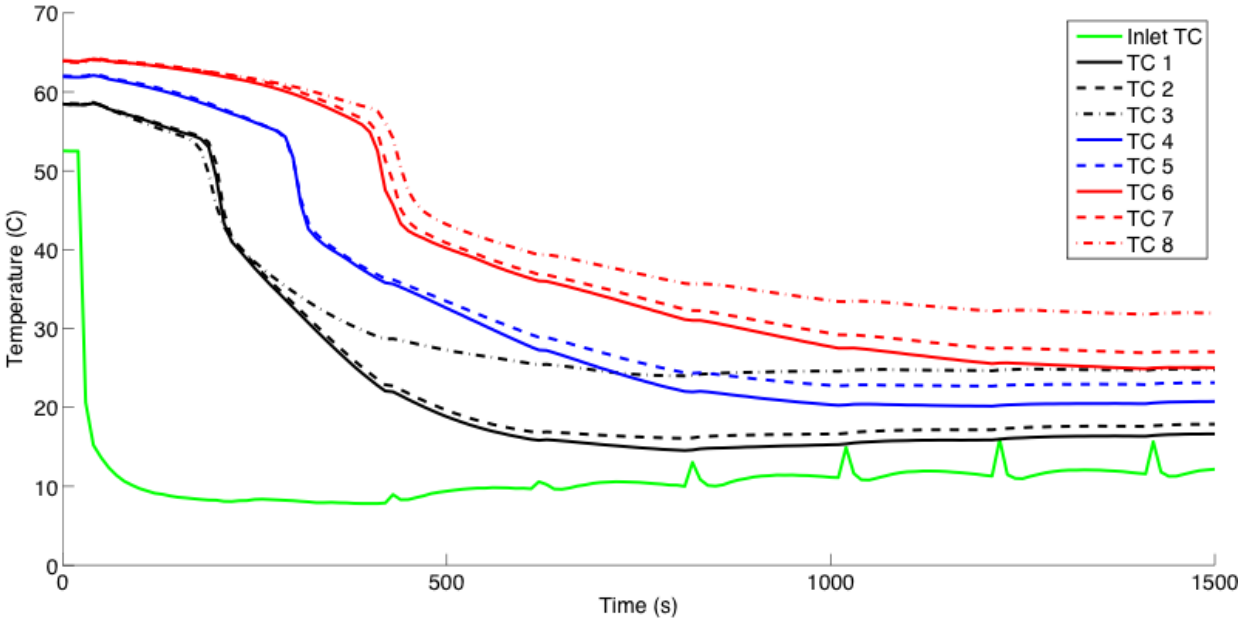

Figure 4: Temperature plot from a representative experimental run, 60℃ initial temperature, 150 ml/min flowrate, 10 MPa (1455 psi) pressure. The lowest line (green) shows the temperature at the fluid injection point. The three groups of lines above that present data from the three axial distances of the thermocouple array, with the lower group plotted in black, representing the thermocouples closest to the inlet, the blue next nearest, and the red representing the farthest. The line style indicates the radial location of the thermocouple. Solid lines indicate that the location is on the axis, the dot dashed lines represent the thermocouples closest to the vessel wall, and the dashed lines represent an intermediate location.

ranged from 50 to 175 ml/min. The experimental Peclet number ranged from 130 to 1,260, with a maximum Reynolds number of 2.56. The flow conditions were well within the Darcy flow regime, but, as expected, our Peclet numbers were three orders of magnitude less than for a field system.

The interplay between advective and diffusive transport can be seen in the shape of the temperature vs. time curves. A purely advective process would feature sharp thermal fronts and a near vertical slope at the time when the cold fluid slug reached the thermocouple. A purely diffusive process would generate a gentler slope with smooth transitions. Our results show that the Peclet number is strongly correlated with the shape of the temperature breakthrough curves (e.g. Fig. 5). It can be seen that the curves in the plots become steeper and less smooth with increasing Peclet number.

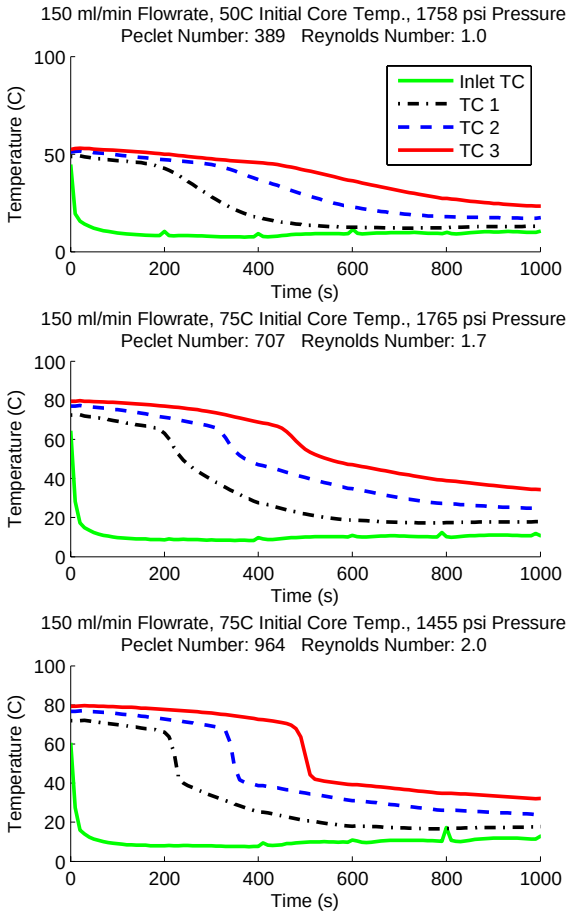

Figure 5: Tests run at a flow rate of 150 ml/min, arranged in order of increasing Peclet number.

A simplified 2-D axisymmetric model of the experimental apparatus was implemented in TOUGH2/ECO2N. The model consisted of 646 grid blocks and assumed a no flux heat boundary at the vessel exterior. The results of the simulation compared to experimental data using the same conditions are shown in Figure 6. The simulations match the experimental results well.

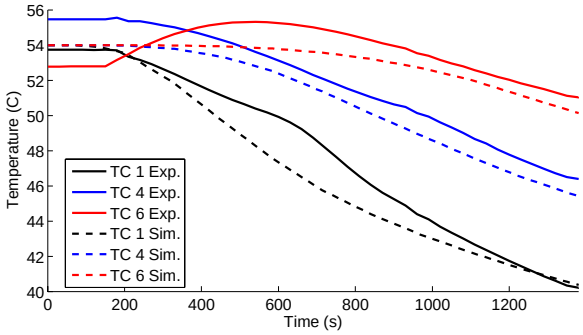

Figure 6: Comparison of experimental and simulated results. Experimental data are plotted with sold lines, simulated plotted with dashed lines.

CONCLUSION

Our laboratory tests are still at an early stage but show great promise. The tests we have conducted so far give us confidence in our numerical model, and provide a great deal of guidance for our next iteration of experiments. One of the principle difficulties experienced with our apparatus was the lack of good control, or accounting of, the mass flow rate into the vessel after the first two pump volumes. A second issue arose from the inability to effectively pump fluid at a rate greater than 150 ml/min which reduced the range of dynamics that could be studied. Both of these problems will be addressed in the future with a combination of a mass flow meter and a more capable pump. Our new design will include the ability to prescribe a mass flow rate for our injected fluid.

ACKNOWLEDGEMENT

This work was supported by the Assistant Secretary for Energy Efficiency and Renewable Energy, Office of Technology Development, Geothermal Technologies Program, of the U.S. Department of Energy under Contract No. DE-AC02-05CH11231.

REFERENCES

Bear, J. (1972), *Dynamics of Fluids in Porous Media*, 764 pp., Dover Publications, New York.

Brown D.W. (2007), "A Hot Dry Rock Geothermal Energy Concept Utilizing Supercritical CO2 Instead of Water." In *Proceedings of the Twenty-Fifth Workshop on Geothermal Reservoir Engineering*, Stanford University, 233-238

Freeze, R. A., and J. A. Cherry (1979), *Groundwater*, 604 pp., Prentice-Hall, Inc.

Liao S.M. and Zhao T.S. (2002), "An experimental investigation of convection heat transfer to supercritical carbon dioxide in miniature tubes", *Int. J. Heat Mass Transfer*, 45, 5025–5034

Majer E.L., Baria R., Stark M., Oates S., Bommer J., Smith B., and Asanuma H. (2007), "Induced seismicity associated with enhanced geothermal systems." *Geothermics*, 36(3):185-222

Pruess, K. (2004), "The TOUGH Codes—A Family of Simulation Tools for Multiphase Flow and Transport Processes in Permeable Media", *Vadose Zone J.*, Vol. 3, pp. 738 – 746

Pruess, K. Enhanced Geothermal Systems (EGS) Using CO2 as Working Fluid – A Novel Approach for Generating Renewable Energy with Simultaneous Sequestration of Carbon, *Geothermics*, Vol. 35, No. 4, pp. 351–367, August 2006.

Pruess, K. (2007), "Enhanced Geothermal Systems (EGS) Comparing Water With CO2 as Heat Transmission Fluids." In *Proceedings, New Zealand Geothermal Workshop 2007 Auckland, New Zealand, November 19-21*

Pruess K. and Spycher N. (2007), ECO2N – A Fluid Property Module for the TOUGH2 Code for Studies of CO2 Storage in Saline Aquifers, *Energy Conv. Mgmt.*, Vol. 48, No. 6, pp. 1761–1767,doi:10.1016/j.enconman.2007.01.016

Pruess, K. and N. Spycher. Enhanced Geothermal Systems (EGS) with CO_2 as Heat Transmission Fluid - A Scheme for Combining Recovery of Renewable Energy with Geologic Storage of CO_2, *Proceedings*, World Geothermal Congress 2010, Bali/Indonesia, 25-29 April 2010.

Tester, J. W., Anderson, B., Batchelor, A., Blackwell, D., DiPippo, R., Drake, E., Garnish, J., Livesay, B., Moore, M. C., Nichols, K., Petty, S., Toksoz, N., Veatch, R., Augustine, C., Baria, R., Murphy, E., Negraru, P., Richards, M., (2006), "The future of geothermal energy: Impact of enhanced geothermal systems (EGS) on the United States in the 21st century", Massachusetts Inst. Technology, DOE Contract DE-AC07-05ID 14517 Final Rept., 374 p.

Xu, T. and K. Pruess. Reactive Transport Modeling to Study Fluid-Rock Interactions in Enhanced Geothermal Systems (EGS) with CO_2 as Working Fluid, *Proceedings*, World Geothermal Congress 2010, Bali/Indonesia, 25-29 April 2010.